Front. Phys., 2014, 9(2): 153–156
DOI 10.1007/s11467-013-0402-0

RESEARCH ARTICLE

Phase regulated suppression and enhancement switches of four-wave mixing and fluorescence

Zhi-Guo Wang, Peng Ying, Pei-Ying Li, Hua-Yan Lan, He-Qing Huang, Hao Tian, Jian-Ping Song, Yan-Peng Zhang†

Key Laboratory for Physical Electronics and Devices of the Ministry of Education & Shaanxi Key Lab of Information Photonic Technique, Xi'an Jiaotong University, Xi'an 710049, China

Corresponding authors. E-mail: †*ypzhang@mail.xjtu.edu.cn*

Received August 23, 2013; accepted October 17, 2013

We experimentally study the phase regulated switch between electromagnetically induced transparency and electromagnetically induced absorption in probe transmission signal and the conversion between enhancement and suppression in four-wave mixing and fluorescence signals for the first time. By changing the relative phase, electromagnetically induced transparency can be converted into electromagnetically induced absorption. In this process, the conversion from suppression to enhancement is also obtained in four-wave mixing and fluorescence signals. This research can be applied in non-linear optical device like optical switch and optical wavelength convertor.

Keywords four-wave mixing, fluorescence, phase regulation, enhancement and suppression

PACS numbers 42.65.-k, 42.50.Gy, 42.62.Fi, 42.65.Jx

1 Introduction

Electromagnetically induced transparency (EIT) system has a very large third-order Kerr nonlinearity effect caused by atomic coherence and little linear absorption [1–3]. Based on these characteristics, four-wave mixing (FWM) signal can be allowed to generate efficiently within the EIT windows [3–6]. Meanwhile, fluorescence signal can also be observed due to the spontaneous emission [3, 7, 8]. Furthermore, the switch between the EIT and electromagnetically induced absorption (EIA) has aroused much concern [9, 10]. It is also reported the conversion between bright state (EIA in probe transmission signal and enhancement in FWM and fluorescence signals) and dark state (EIT in probe transmission signal and suppression in FWM and fluorescence signals) can be realized by changing the dressing field power and the frequency detunings of incident laser fields [9, 11, 12]. Besides, some experimental and theoretical studies have demonstrated the switch between bright and dark states caused by the regulated phase difference between the two circularly polarized components of a single coherent field [13].

In this paper, we experimentally investigate the EIT/EIA switch and the conversion between enhancement and suppression of FWM and fluorescence signals by the phase modulation for the first time. We firstly realize the conversion between bright and dark states by modulating the relative phase in ladder type subsystem. Then we consider the phase modulation in a Y-type subsystem. Lastly, the dependence of the signal intensities on the relative phases is given out. Different from other researches [3–5], we explore a new technique to directly observe the dressing effects in the experiment, which is to change the probe field frequency detuning as the coupling field frequency detuning is scanned. Further, we can use this technique to observe the switch of dressing effects.

2 Experimental scheme and theoretical model

Our experiment is carried out in a rubidium atomic vapor cell, where the relevant energy levels $5S_{1/2}$ ($|0\rangle$), $5P_{3/2}$ ($|1\rangle$), $5D_{5/2}$ ($|2\rangle$) and $5D_{3/2}$ ($|3\rangle$) constitute a four-level Y-type atomic system, as shown in Fig. 1(a). The lower transition $|0\rangle$ to $|1\rangle$ is probed by a weak probe laser beam E_1 whose frequency is ω_1 and wave vector is $\boldsymbol{k}_1$. Two coupling laser beams E_2 (ω_2, $\boldsymbol{k}_2$) and E_2' (ω_2, $\boldsymbol{k}_2'$) drive the upper transition $|1\rangle$ to $|2\rangle$. Another two coupling laser beams E_3 (ω_3, $\boldsymbol{k}_3$) and E_3' (ω_3, $\boldsymbol{k}_3'$) connect the other upper transition $|1\rangle$ to $|3\rangle$. In normal experiment, we place the five laser beams in a square-box pattern as shown

in Fig. 1(b). All the coupling beams E_2, E_2', E_3 and E_3' propagate through the Rb vapor cell in the same direction and the angles between any two are about 0.3°. The probe field E_1 propagates in the opposite direction of E_2. Here we study phase modulation switch and the normal experimental configuration will be revised. The coupling fields E_2 and E_2' are deviated from the normal position with an angle α as shown in Fig. 1(c). In our experimental system, the FWM signals generated by E_1, E_3 and E_3' in ladder-type $|0\rangle-|1\rangle-|3\rangle$ subsystem and by E_1, E_2 and E_2' in $|0\rangle-|1\rangle-|2\rangle$ subsystem are called E_{F1} and E_{F2}, respectively. In addition, we use R_0 to represent the single-photon fluorescence signal generated from $|1\rangle$ to $|0\rangle$. R_1 and R_2 denote two-photon fluorescence signals from $|3\rangle$ to $|1\rangle$ and from $|2\rangle$ to $|1\rangle$, respectively.

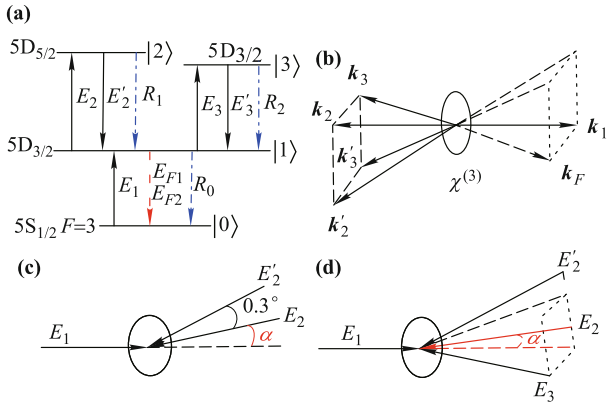

Fig. 1 **(a)** Relevant ^{85}Rb four-level atomic system. **(b)** Normal phase-matching configuration with $\boldsymbol{k}_2$ propagating in the opposite direction of $\boldsymbol{k}_1$. **(c, d)** Abnormal configurations for ladder type subsystem and Y-type system with the deflection angle α.

In general, we can acquire the density matrix elements $\rho_{10}^{(1)}$ (related to EIT), $\rho_{10}^{(3)}$ (related to FWM signal), and $\rho_{11}^{(2)}$, $\rho_{22}^{(4)}$ and $\rho_{33}^{(4)}$ (related to fluorescence signals) by solving the coupled density-matrix equations. With the Liouville pathway $\rho_{00}^{(0)} \xrightarrow{E_1} \rho_{10}^{(1)}$ and considering the dressing effect of E_2 and E_3, we can obtain $\rho_{10DD}^{(1)} = \mathrm{i}G_1/(d_1 + |G_2|^2\mathrm{e}^{\mathrm{i}\Delta\Phi}/d_2 + |G_3|^2/d_3)$ (the subscript DD means double dressing), where $d_1 = \Gamma_{10}+\mathrm{i}\Delta_1$, $d_2 = \Gamma_{20}+\mathrm{i}(\Delta_1+\Delta_2)$, $d_3 = \Gamma_{30}+\mathrm{i}(\Delta_1+\Delta_3)$, $\Delta_i = \Omega_i-\omega_i$ (Ω_i represents the level resonance frequency and Γ_{ij} represents the transverse relaxation rate between states $|i\rangle$ and $|j\rangle$). Besides, we have introduced an additional phase factor $\mathrm{e}^{\mathrm{i}\Delta\Phi}$ ($\Delta\Phi$ is related with the orientations of induced dipole moments μ_1 and μ_2 [14]) into the dressing term $|G_2|^2/d_2$ in $\rho_{10\mathrm{DD}}^{(1)}$ when considering the angle α between E_2 and the opposite direction of E_1. For FWM signal E_{F1}, the element $\rho_{F1\mathrm{DD}}^{(3)}$ can be expressed as $\rho_{F1DD}^{(3)} = -\mathrm{i}G_1G_2(G_2')^*/[(d_1 + |G_2|^2\mathrm{e}^{\mathrm{i}\Delta\Phi}/d_2 + |G_3|^2/d_3)^2d_2]$ via the Liouville pathway $\rho_{00}^{(0)} \xrightarrow{E_1} \rho_{10}^{(1)} \xrightarrow{E_2} \rho_{20}^{(2)} \xrightarrow{(E_2')^*} \rho_{10}^{(3)}$. Via the Liouville pathway $\rho_{00}^{(0)} \xrightarrow{E_1} \rho_{10}^{(1)} \xrightarrow{(E_1)^*} \rho_{11}^{(2)}$, The single-photon fluorescence R_0 can be obtained as $\rho_{11DD}^{(2)} = -|G_1|^2/[\Gamma_{11}(d_1 + |G_3|^2/d_3 + |G_2|^2\mathrm{e}^{\mathrm{i}\Delta\Phi}/d_2)]$ with doubly dressing effect. By the pathway $\rho_{00}^{(0)} \xrightarrow{E_1} \rho_{10}^{(1)} \xrightarrow{E_2} \rho_{20}^{(2)} \xrightarrow{(E_1)^*} \rho_{21}^{(3)} \xrightarrow{(E_2)^*} \rho_{22}^{(4)}$, we can also obtain $\rho_{22SD}^{(4)} = |G_1|^2|G_2|^2/[\Gamma_{22}d_1d_4(d_2 + |G_2|^2\mathrm{e}^{\mathrm{i}\Delta\Phi}/d_1)]$ (the subscript SD means single dressing) and $\rho_{22DD}^{(4)} = |G_1|^2|G_2|^2/[\Gamma_{22}d_1d_4(d_2+|G_2|^2\mathrm{e}^{\mathrm{i}\Delta\Phi}/(d_1+|G_3|^2/d_3))]$ representing the single dressing and double dressing two-photon fluorescence R_1, respectively.

3 Analysis and discussion of experimental results

First of all, we concentrate on the phase regulated switch in ladder type subsystem, as shown in Fig. 2, where we scan Δ_2 at different discrete Δ_1 with $\Delta\Phi = -\pi/5$ [Fig. 2(a)] and $\Delta\Phi = 3\pi/5$ [Fig. 2(b)]. In Fig. 2(a1), we can find that EIT peaks appear at negative detunings. With the detunings turned from negative to positive, the probe transmission signal is converted from EIT to partial-EIT-partial-EIA and lastly to EIA. However, in Fig. 2(b1), EIA dips emerge at negative detunings and the EIT peaks appear at positive detunings, which is opposite to the case of $\Delta\Phi = -\pi/5$ due to the modulation of the phase factor $\mathrm{e}^{\mathrm{i}\Delta\Phi}$ in the dressing term $|G_2|^2\mathrm{e}^{\mathrm{i}\Delta\Phi}/d_2$ in $\rho_{10DD}^{(1)}$. In Fig. 2(a2), we can easily find that the FWM signals at negative detunings are much stronger than that at positive detunings because the transition possibility at negative detunings is much bigger than that at positive detunings. By comparing Fig. 2(b2) with Fig. 2(a2), we can see that the FWM signals become obviously weaker, which is the reason that the incident light angle has larger deviation from the normal position and the interaction region of the probe field and the coupling field becomes smaller. The fluorescence signal [Figs. 2(a3) and (b3)] is made up of the single-photon fluorescence R_0 and two-photon fluorescence R_1. The dip shows the suppression on R_0 owing to the dressing effect of E_2, which is corresponding to EIT. The peak in the dip represents fluorescence R_1, which is corresponding to EIA. In Fig. 2(a3), with $|\Delta_1|$ increasing, on one hand, the dip (induced by the dressing term $|G_2|^2\mathrm{e}^{\mathrm{i}\Delta\Phi}/d_2$ in $\rho_{11\mathrm{SD}}^{(2)}$) becomes inconspicuous due to the reduced dressing effect of E_2, and on the other hand, the peak (R_1) becomes strong due to the attenuate suppression induced by the dressing term $|G_2|^2\mathrm{e}^{\mathrm{i}\Delta\Phi}/d_1$ in $\rho_{22\mathrm{SD}}^{(4)}$. When the phase switches from $-\pi/5$ to $3\pi/5$, the peaks become higher since the dressing effect induced by $E_2(E_2')$ on R_1 changes from suppression (in correspondence with EIT)

to enhancement (in correspondence with EIA). Meanwhile, the dips become shallower owing to the weakened dressing effect of $E_2(E_2')$ on R_0 at $\Delta\Phi = 3\pi/5$. Figures 2(c) and (d) are the corresponding calculated results, agreeing with Figs. 2(a) and (b) very well, respectively.

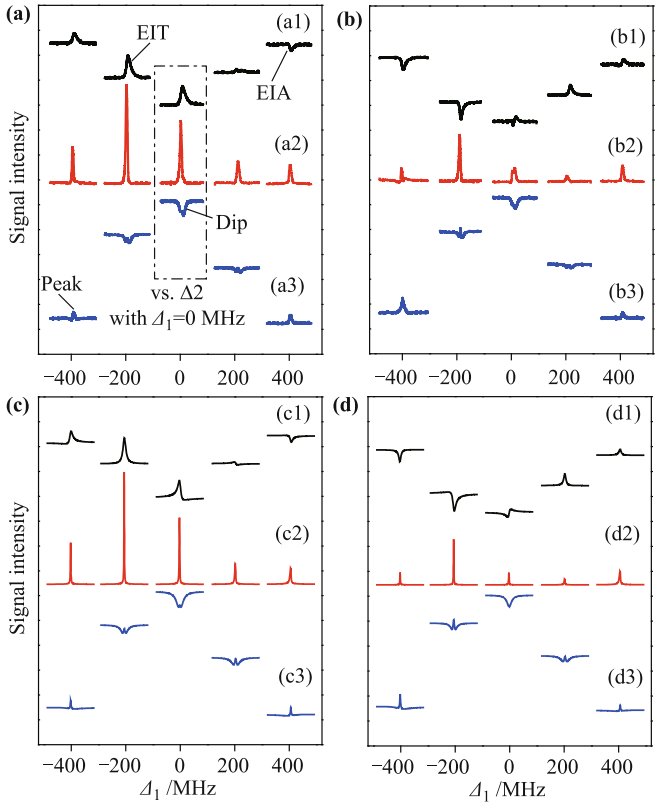

Fig. 2 Measured probe transmission signals **(a1, b1)**, FWM signals **(a2, b2)** and fluorescence signals **(a3, b3)** versus Δ_2 with E_3 and E_3' blocked when Δ_1 is set at different discrete detunings. For (a1)–(a3) $\Delta\Phi = -\pi/5$ and for (b1)–(b3) $\Delta\Phi = 3\pi/5$. The other parameters are $P_1 = 7.8$ mW, $P_2 = 2.3$ mW, $P_2' = 4.8$ mW. **(c, d)** The calculated curves corresponding (a, b), respectively.

In the following, we turn our interest to the phase regulated switch in Y-type subsystem. With E_1, E_2, E_2' and E_3 turned on and E_3' blocked, we obtain the signals by scanning Δ_2 at different discrete Δ_1 with $\Delta\Phi = 0$ [Fig. 3(a)] and $\Delta\Phi = 3\pi/4$ [Fig. 3(b)]. In the probe transmission spectrum [Figs. 3(a1) and (b1)], the peak higher than the baseline of each curve means the $|0\rangle - |1\rangle - |2\rangle$ EIT and the dip lower than the baseline represents the $|0\rangle - |1\rangle - |2\rangle$ EIA. The $|0\rangle - |1\rangle - |3\rangle$ EIT is denoted by the peak of the global profile formed from the baselines. By comparing the curves at $\Delta_1 + \Delta_3 = 0$, –15 and –30 MHz, we can find that both the $|0\rangle - |1\rangle - |2\rangle$ EIT in Fig. 3(a1) and the $|0\rangle - |1\rangle - |2\rangle$ EIA in Fig. 3(b1) arrive at their smallest amplitude at $\Delta_1 + \Delta_3 = 0$. This is because the external dressing term $|G_3|^2/d_3$ induced by $E_3(E_3')$ in $|0\rangle - |1\rangle - |3\rangle$ subsystem has suppression on the $|0\rangle - |1\rangle - |2\rangle$ EIT (or EIA), which are expressed as $d_1 + |G_2|^2/d_2 + |G_3|^2/d_3$ in $\rho_{10DD}^{(1)}$. When $\Delta\Phi = 0$, most of the curves in the probe transmission spectrum are presented as EIT. While the relative phase turned to $3\pi/4$, a majority of the curves change from EIT to EIA. In this process, the FWM signals become stronger for that the suppression effect on FWM signals comes with EIT and the enhancement effect comes with EIA. For fluorescence signals in Y-type subsystem [Figs. 3(a3) and (b3)], as a result of the suppression induced by the dressing term $|G_3|^2/d_3$ on R_0 in $\rho_{11DD}^{(2)}$, the profile consisting of their baselines reaches its minimum at $\Delta_1 + \Delta_3 = 0$. The peaks in the dips [Figs. 3(a3) and (b3)] represent the two-photon fluorescence signals R_1 ($\rho_{22DD}^{(4)}$). In Y-type subsystem, we can also find the peaks in fluorescence signals get higher and dips get shallower with $\Delta\Phi$ changed from 0 to $3\pi/4$, which is for the same reason with that in Fig. 2.

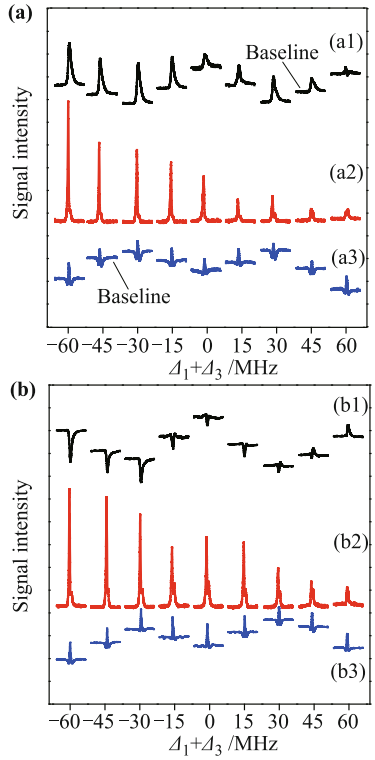

Fig. 3 Measured probe transmission signals **(a1, b1)**, FWM signals **(a2, b2)** and fluorescence signals **(a3, b3)** versus Δ_2 with E_3' blocked and $\Delta_3 = 110$ MHz when Δ_1 is set at different discrete detunings. For (a1)–(a3) $\Delta\Phi = 0$, and for (b1)–(b3) $\Delta\Phi = 3\pi/4$. The other parameters are $P_1 = 7.8$ mW, $P_2 = 6.9$ mW, $P_2' = 15.9$ mW and $P_3 = 46.1$ mW.

Finally, we focus on the dependence of the signal intensities on the relative phases $\Delta\Phi$. With E_3 and E_3' blocked, the signals are obtained with the phase $\Delta\Phi$ continuously altered, as shown in Fig. 4. When the relative

phase $\Delta\Phi$ changes from $7\pi/6$ to $2\pi/3$, the probe transmission signal transforms from weak EIA to strong EIA, and then to weak EIA again. When we continue altering the phase, a weak EIT appears, then turns to strong EIT and finally to weak EIT. In this process, the FWM signal peak in Fig. 4(b) becomes higher and reaches its maximum at $\Delta\Phi = 2\pi/3$ due to the enhancement caused by $E_2(E_2')$ and then the FWM signal monotonically decreases for that the original enhancement effect turns to suppression effect with $\Delta\Phi$ continuously changing. In the fluorescence signals [Fig. 4(c)], the depth of the dip reaches the maximum at $\Delta\Phi = 0$ on account of the biggest EIT. Similarly, the peak of the two-photon fluorescence R_1 induced by $E_2(E_2')$ become highest at $\Delta\Phi = \pi$ owing to the strongest EIA.

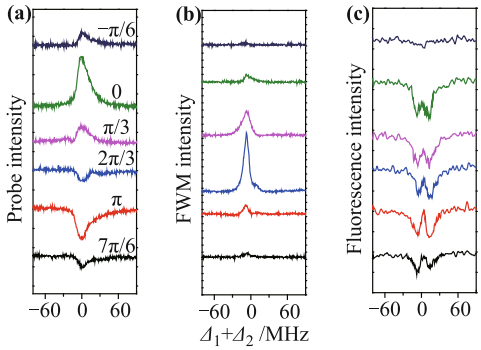

Fig. 4 Measured probe transmission signals **(a)**, FWM signals **(b)**, and fluorescence signals **(c)** versus Δ_2 with $\Delta\Phi = 7\pi/6$, π, $2\pi/3$, $\pi/3$, 0 and $-\pi/6$ from bottom to top when E_3 and E_3' blocked. The other parameters are $P_1 = 4.8$ mW, $P_2 = 7.8$ mW, $P_2' = 7.3$ mW and $\Delta_1 = -120$ MHz.

4 Conclusion

In conclusion, we have demonstrated the phase regulated switch. It has been observed in our experiment that the suppression in FWM and fluorescence signals is converted into enhancement in correspondence with the switch from EIT to EIA with the relative phase altered from 0 to $3\pi/4$. We can make use of the phase regulated switch in non-linear optical device like optical switch and optical wavelength convertor. Moreover, such phase controlled switch could have potential applications in optical communication and quantum information processing when utilized in solid material such as Pr-doped YSO crystals.

Acknowledgements The work was supported by the National Basic Research Program (973 Program) (Grant No. 2012CB921804), the National Natural Science Foundation of China (Grant Nos. 10974151, 61078002, 61078020, 11104214, 61108017, 11104216, and 61205112), the Program for New Century Excellent Talents in University (NCET) (Grant No. 08-0431), RFDP (Grant Nos. 20110201110006, 20110201120005, and 20100201120031), the Fundamental Research Funds for the Central Universities (FRFCU) (Grant Nos. 2012jdhz05, 2011jdhz07, xjj2011083, xjj2011084, xjj20100151, xjj20100100, and xjj2012080), and CPSF (Grant No. 2012M521773).

References and notes

1. M. Kash, V. Sautenkov, A. Zibrov, L. Hollberg, G. Welch, M. Lukin, Y. Rostovtsev, E. Fry, and M. Scully, Ultraslow group velocity and enhanced nonlinear optical effects in a coherently driven hot atomic gas, *Phys. Rev. Lett.*, 1999, 82(26): 5229
2. S. Wielandy and A. Gaeta, Investigation of electromagnetically induced transparency in the strong probe regime, *Phys. Rev. A*, 1998, 58(3): 2500
3. S. E. Harris, Electromagnetically induced transparency, *Phys. Today*, 1997, 50(7): 36
4. B. S. Ham, M. S. Shahriar, and P. R. Hemmer, Enhanced nondegenerate four-wave mixing owing to electromagnetically induced transparency in a spectral hole-burning crystal, *Opt. Lett.*, 1997, 22(15): 1138
5. D. Braje, V. Balic, S. Goda, G. Yin, and S. Harris, Frequency mixing using electromagnetically induced transparency in cold atoms, *Phys. Rev. Lett.*, 2004, 93(18): 183601
6. Z. K. Wu, Y. Q. Zhang, T. K. Liu, Z. Y. Zhang, C. Li, Y. P. Zhang, and M. Xiao, Coherent control of dressed images of four-wave mixing, *Front. Phys.*, 2013, 8(2): 228
7. J. Qi, G. Lazarov, X. Wang, L. Li, L. M. Narducci, A. M. Lyyra, and F. C. Spano, Autler–Townes splitting in molecular lithium: Prospects for all-optical alignment of nonpolar molecules, *Phys. Rev. Lett.*, 1999, 83(2): 288
8. J. Qi and A. M. Lyyra, Electromagnetically induced transparency and dark fluorescence in a cascade three-level diatomic lithium system, *Phys. Rev. A*, 2006, 73(4): 043810
9. N. Li, Z. Zhao, H. Chen, P. Li, Y. Li, Y. Zhao, G. Zhou, S. Jia, and Y. Zhang, Observation of dressed odd-order multi-wave mixing in five-level atomic medium, *Opt. Express*, 2012, 20(3): 1912
10. A. M. Akulshin, S. Barreiro, and A. Lezama, Electromagnetically induced absorption and transparency due to resonant two-field excitation of quasidegenerate levels in Rb vapor, *Phys. Rev. A*, 1998, 57(4): 2996
11. Z. Wang, Y. Zhang, H. Zheng, C. Li, F. Wen, and H. Chen, Switching enhancement and suppression of four-wave mixing via a dressing field, *J. Mod. Opt.*, 2011, 58(9): 802
12. C. Li, H. Zheng, Y. Zhang, Z. Nie, J. Song, and M. Xiao, Observation of enhancement and suppression in four-wave mixing processes, *Appl. Phys. Lett.*, 2009, 95(4): 041103
13. U. Khadka, Y. P. Zhang, and M. Xiao, Control of multitransparency windows via dark-state phase manipulation, *Phys. Rev. A*, 2010, 81(2): 023830
14. K. H. Hahn, D. A. King, and S. E. Harris, Nonlinear generation of 104.8-nm radiation within an absorption window in zinc, *Phys. Rev. Lett.*, 1990, 65(22): 2777